Chemo-rheological studies and monitoring of high-Tg reactive polyphtalamides towards a fast innovative RTM processing of fiber-reinforced thermoplastic composites

M. Dkier, Mohammed Yousfi, K. Lamnawar, A. Maazouz

Chemo-rheological studies and monitoring of high-Tg reactive polyphtalamides towards a fast innovative RTM processing of fiber-reinforced thermoplastic composites

M. Dkier[a], M. Yousfi[a], K. Lamnawar[a*], A. Maazouz[a,b*]

[a]Université de Lyon, , INSA Lyon, CNRS, UMR 5223, Ingénierie des Matériaux Polymères, F-69621 Villeurbanne, France
[b] Hassan II Academy of Science and Technology, 10 100 Rabat, Morocco

*Correspondin author: khalid.lamnawar@insa-lyon.fr, abderrahim.maazouz@insa-lyon.fr

Abstract

In this work, a High Temperature hybrid process coupling “reactive Extrusion” and “Resin Transfer Molding” (HT-ERTM) was designed for the manufacturing of continuous Glass Fiber-Reinforced Thermoplastic Composites (GFRTC) with an elevated glass transition temperature. Hereto, a high-performance polyphtalamide (PPA) obtained from the chain extension reaction of its prepolymer was studied with the optimal stoichiometry ratio and at several temperatures. Due to the extremely fast reaction, the present work highlights that both the reaction kinetics and the increase in viscosity are not easily monitored at short times and at high temperatures by usual techniques such as DSC and titration methods. The chemo-rheological evolutions were first studied ex-situ by coupling rheology with fast scan FTIR. In a second step, the HT-ERTM process was equipped with specific dielectric sensors in order to in-situ track the reaction evolution and the flow properties up to injection inside the cavity. Meanwhile, the viscosity increase was then determined depending on time, temperature and molar mass growth. Specifically, it was possible to model its evolution at less than one minute whereas the reaction conversion reaches 85% on two minutes of processing window. Interestingly, it was found that the in-situ results corroborated their ex-situ counterparts mentioned above. Finally, GFRTC parts with fiber contents up to 60 wt. % were obtained with a better control of both mechanical and thermo mechanical properties intended especially for high service temperature applications such as in the automotive or aerospace industries.

Keywords: Hybrid TP-RTM, rheokinetics, composites, in-situ monitoring.

1. Introduction

Nowadays, composites based on high-performance thermoplastic (TP) matrices have become particularly attractive in many industries, e.g., the aerospace and automotive sectors [1]. Because of their good mechanical resistance (intrinsic ductility and tenacity), their low environmental impact (ecofriendly production method, recycling), their potential to reduce the production cycle (thus a greater production capacity) and their welding properties, they strongly compete with composites based on a thermosetting matrix [2, 3]. However, the excessively high viscosity of the TP in the molten state makes it extremely difficult to produce continuous fiber-reinforced composites by injection at pressure lower than 15 bar and especially when the fiber content is high (≥30 vol%), as required for structure parts applications [4]. An alternative approach consists in using the TP matrices from monomers or prepolymers in a reactive processing route conventionally used for thermosetting matrices [5]. Among the methods available for the manufacturing of these materials, RTM (Resin Transfer Molding) makes it possible to obtain composite parts by injecting a low-viscosity resin onto pre-formed continuous fiber reinforcements in a mold. This process is undergoing rapid development because of its "closed mold" technology as well as the wide range of parts with complex shapes that become available. During the last decade, the idea of adapting the RTM process to make TP-based composites has awoken interest among scientists [6]. However, the choice of the thermoplastic matrix depends on the intended application. At present, the development of this new process has begun with specific polymers for which the chemistry is much more controlled. The constraints related to the manufacturing conditions, the polymerization and the concomitant crystallization therefore make it possible to consider only a relatively limited number of TP matrices. Despite the interesting literature dedicated to the composite field, it is a daunting task for both scientific and industrial communities to adapt RTM process to these new generation of TP fiber-reinforced composites. Indeed, many routes have been investigated involving bi or mono-reactive component to form a TP matrix up to the impregnation. On one hand, structural reaction injection molding (SRIM) uses high pressure (8–10 bar) to impregnate a dry fiber preform, which is placed between two solid mold halves. The process is closely related to the classical RTM of thermoset composites. In order to obtain a good fiber impregnation, 1 Pa.s is generally regarded as the maximum viscosity limit of the reactive system. Upon completion of polymerization, the composite part can be demolded. On the other hand, vacuum infusion (VI) is also employed to compact and impregnate a dry and continuous fiber preform, which is placed between a solid and a flexible mold half. After mixing the contents of the two material tanks, the reactive system (viscosity: less than 1 Pa.s) is dispensed into a buffer vessel, which is required to separate the pressure required for dispensing and the vacuum necessary to promote infusion. The required time is generally longer than SRIM technology. Commingled yarns are one of the possible preforms used for continuous fiber reinforced thermoplastic composites in order to solve the problem of high melt viscosity during impregnation and consolidation steps. The tradename TWINTEX® is one commercial reference and it's a unidirectional thermoplastic/glass fiber composites prepared from an online combination of commingled E-glass and polypropylene filaments [7]. Due to the high melt viscosity of the thermoplastic polymer matrix, commingled yarn spinning process is considered one of the most promising impregnation techniques since a homogeneous distribution of continuous matrix filaments and reinforcement glass filaments took place during melt spinning. However, this technique should be improved for high Tg engineering polymers.

Furthermore, the literature includes reports relating to the physicochemical study of TP formulations based mainly on c-PBT [8], PA6 [9], PA12 [10] and PMMA [11] for RTM applications or other processes such as pultrusion [12], infusion [13], RIM [14] and LCM [15]. Pultrusion [20] and SRIM like processes [16, 18, 21] for TP based composites have intensively been developed in the past decade**.** The authors generally emphasize the interest of adapting the nature of the monomers/prepolymers (which influences the kinetics of polymerization) to the size of the parts to be manufactured (for thick parts one should favor a slower reaction to obtain good

impregnation). Glass and/or carbon fiber-reinforced composite parts have been characterized by numerous authors in terms of fiber content, crystallinity, melting point of the matrix and for two different thermal cycles [14]. In particular, Mairtin et al. [16] found some sensitivity of PA12-based systems to humidity and the importance of having a good fiber-matrix interface and a better control of its impregnation. Luisier et al. [17] plotted a TTT (Time - Temperature - Transformation) diagram of PA12 in which a processing window was proposed. Zingraff et al. [18] studied the problem of forming voids in the composite (in and between wicks) in order to optimize the impregnation in the RTM process. Hakme et al. [19] reported on a competition between in-situ reaction of butylene terephthalate (CBT) oligomers and crystallization of the obtained c-PBT. The literature shows that the physicochemistry of some of these TP polymers has been widely studied. More specifically, Ageyeva et al. [22] has recently summarized in a review article the literature data devoting to the use of TTT diagrams in the case of TP-RTM processing. Such diagrams have been developed for the PA12 reactive system [17] and for the PA6 reactive system [23]. Despite the interesting kind of research dedicated to this subject, there are few papers which the subject is on the topic of the present work involving on high Tg polyamide based composites for fast RTM process. It is always challenging to adapt the usual technologies to intermediate viscous reactive monomers/prepolymers (close to 1 Pa.s) and especially with fast reactive systems. Indeed, the published reports in the last decade deal with systems that have a relatively known and simple chemistry and a service temperature in the range of 50 to 90 °C. Therefore, this class of materials cannot be used in most conventional automotive process chains or for other high performance applications. For example, the composite parts need to resist to the high temperature imposed during the cataphoresis treatment in which a maximum temperature of about 190 °C could be encountered [24]. Among the promising engineering polymers in these applications, we take note of the emergence of polyphtalamides (hereafter referred to as PPAs) which are considered as high-performance thermoplastic matrices with excellent mechanical and thermal properties. Compared to aliphatic and other classical polyamides, PPAs are typically distinguished by their higher melting points, higher glass transition temperatures and greater dimensional stability [25]. ARKEMA has developed and patented [26, 27] a number of polyphtalamide compositions making it possible to address the development of TP-RTM technology with high-performance polyphtalamides. The principle is to inject the prepolymer of low viscosity (~2.5 Pa.s) mixed with some reactive co-agent (~0.5 Pa.s) into a mold containing the reinforcement (glass or carbon). The temperature is then increased a few tens of degrees above the prepolymer melting temperature. Currently, the monitoring and modeling of a chemical reaction during this processing is a big challenge for scientists and industrial communities [28]. Therefore, on-line process control with in-mold sensors is often used in industrial manufacturing of RTM parts. In-line systems such as dielectric sensors [19], ultrasound transducers [29] and point-voltage sensors [30] can be employed for this purpose. The advancement of a polymerization results in an increase in viscosity so the viscosity of the initial system must not exceed 1 Pa.s to ensure a good filling of the mold in which a porous and continuous reinforcement has been placed. The chemical reaction in the mold is accompanied by a viscosity increase of up to 1000 Pa.s in few minutes. Thus, the challenge lies in the need to characterize this rheological evolution during the first seconds to control and optimize the time required to inject the reactive system into the mold and thus also the impregnation of the reinforcement. Hence, the use of non-destructive and non-invasive methods such as ultrasound or dielectric spectroscopy should be a suitable route to attain this objective. The second scientific constraint that needs to be overcome relates to the adaptation of the devices to the high temperatures which these chemical reactions take place (molding temperatures ranging from 270 to 300 °C). These high processing temperatures implies to have a better choice of the fiber sizing and the interface/interphase properties with the formed matrix. The optimization and modeling of a manufacturing process require the design of an instrumented mold to monitor, in real time and in situ, the progress of the reaction and the resultant phase transformations. Indeed, the structural

evolution of the reactive system is influenced by process parameters such as temperature, time and impregnation flow rate.
The present work proposes the use of a so-called “chain-extender”, which can react with the polyphtalamide prepolymer in the melt at a higher temperature. Consequently, this chain extender can potentially increase the molar masses of PPA within a short time. Firstly, the fast track of the viscosity increase and conversion will be also investigated by ex-situ fast scan FTIR/SAOS measurements. Secondly and to achieve the process control, in-situ monitoring by dielectric sensors will be performed [31, 32]. The dielectric response will be combined with reference models. Then, the fast in-situ monitoring can then be compared to ex-situ measurements. The challenge is to convert the conductivity (from dielectric sensors) to the measured (even modelled) ex-situ resin viscosity (η) of the system towards monitoring of the reaction’s advancement and the structure evolution of the matrix within the fabric. However, the difficulty lies in how to monitor the fast chain extension reaction inside the cavity at short times of polymerization (less than two minutes) in the presence of a high-temperature polymer such as PPA. Indeed, the difference in the melting temperature between the two components of the reaction (PPA prepolymer and the chain extender) leads to the choice of a confined geometry to ensure a good reliability of the monitoring results. The relevance of this approach is that data of the most important process milestones can be reliably generated from the dielectric sensors in real-time throughout the fabrication process. This data includes the injectability limit for the impregnation of the reinforcement and the maximum conversion rate reached by the system. In this study, titration analyses and chemo-rheology coupled to FTIR spectroscopy were also carried out for calibration. The obtained results will be discussed also in term of physico-chemical, morphological and mechanical properties of studied PPA matrix and its corresponding composites.

2. Experimental section

2.1 Materials

The reaction medium consisted of 2 components: a semi-crystalline prepolymer kindly supplied by Arkema (France). This thermoplastic prepolymer [27] is a polyphtalamide (PPA) type PA 10T/11/6T with di-acid chain ends (a content of COOH terminal groups of 0.9 meq/g), obtained by polycondensation at 250°C of 1,6 hexanediamine, 1,10 decanediamine and terephthalic acid in the presence of undecanoic acid. Its chemical formula is shown in Figure 1.

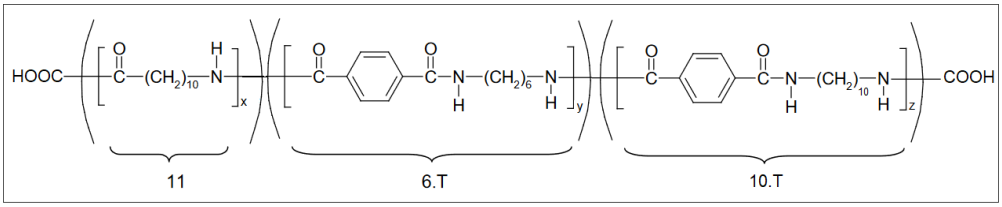

Figure 1*. Chemical structure of the prepolymer used in this study [27].*

The chain extender agent used in this study was 1, 3 phenylene bis-2oxazoline (PBO), denoted “CA” throughout the paper, and was supplied from Evonik (Germany). The essential properties and characteristics of the materials used in this study are listed in Table 1. The prepolymer and chain extender (in solid form) were accurately dried under vacuum for 12h at 80°C and 50°C respectively.

It’s important to remind than the main challenge is to develop a fast manufacturing of PPA based composites as patented [27]. There are few chain extenders dedicated to this target. With ARKEMA group, we have studied other chain extender as well di-epoxy molecules which the reaction kinetics was demonstrated to be equivalent but the mechanical performances of the final PPA matrix was less performant than the chosen PBO system.

***Table 1**: Main characteristics of the prepolymer and the chain extender agent. $\bar{M}_n$: number average molecular weight. T_g: glass transition temperature. T_m: melting temperature. η_0: zero shear viscosity measured in the lab with a cone-plate geometry, 2°.*

Product	$\bar{M}_n$ (g.mol^{-1})	η_0[a] (Pa.s)	T_g (°C)	T_m (°C)
Prepolymer	2700	2.5	100	270
Chain extender	216	0.2	-	150

[a]: *at 280°C for the prepolymer and 180°C for CA chain extender.*

The reaction scheme between the prepolymer and chain extender is presented in Figure 2. The reaction mechanism involved chain lengthening between an acidic prepolymer and a bis-oxazoline. It occurred precisely between the acid/oxazoline functions and resulted in the formation of an esteramide bond at the heart of the formed chain. 1,3 phynelene bis-oxazoline (CA) groups are well known to afford quantitative conversion of carboxylic acids both in melt and solution processes [33]. Indeed, oxazoline groups, which react very quickly with the carboxylic end groups, have proven to be effective in achieving linear chain extension of the polymer by forming stable bis-amide bridging segments (Figure 2a). This linear chain extension reaction yields esteramides quantitatively without formation of any byproducts [34]. Moreover, it has been shown in the literature [35] that the chain extender agent can also react with the amide section as described in Figure 2b. Thus, using a high concentration of 'CA' could lead to the formation of branched chains. In this study, an appropriate iso-stoichiometry ratio between chain extender and prepolymer was determined. For the clarity purpose of the present paper, it was unchanged throughout this work.

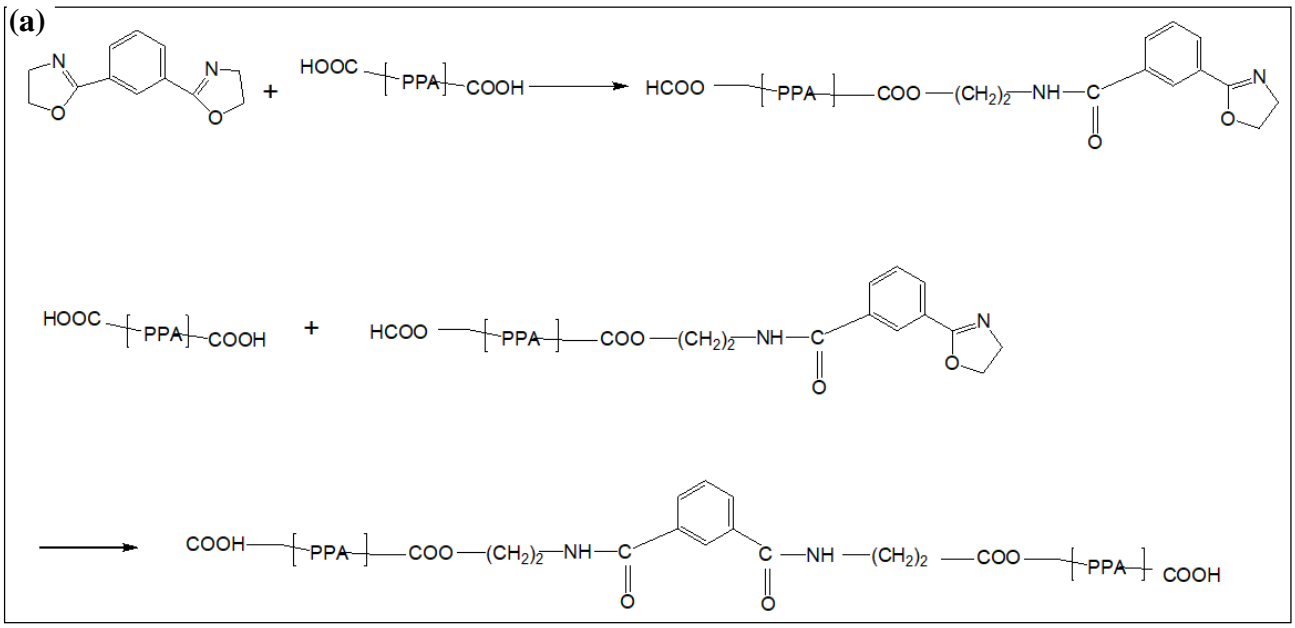

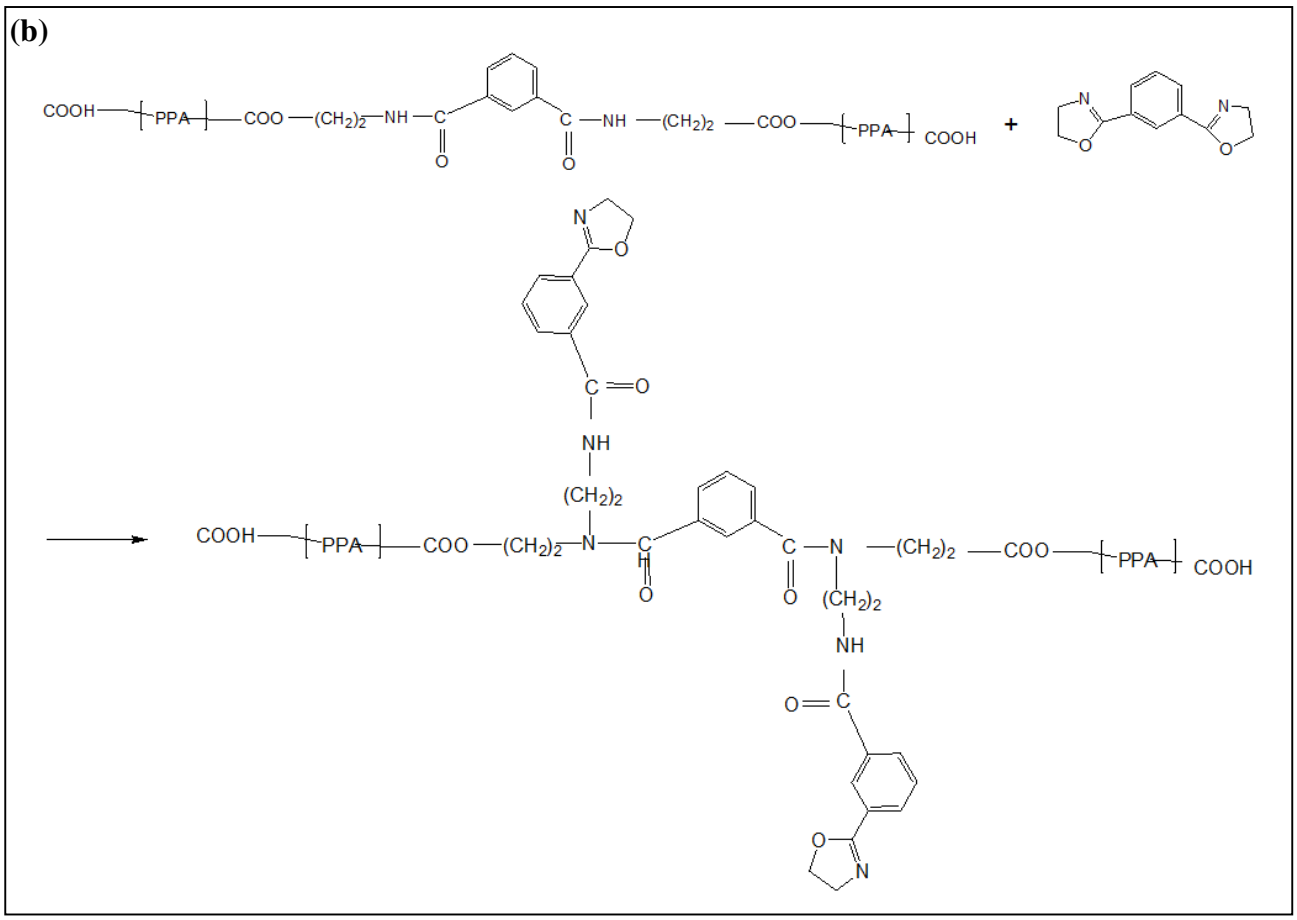

Figure 2. *Reaction mechanism for 1, 3 phenylene bis-oxazoline and carboxylic acid: polymerization via chain extension reaction (scheme a) and possible secondary branching reaction especially at high CA content (scheme b).*

2.2 Reinforcing glass fibers

Woven glass fibers used in this study consisted of a taffeta weave fabric (reference TV 1184) supplied by Hexcel. The reinforcement has a specific weight area of 240 g/m^2 and a ply thickness of 200 µm. The choice of a plain fabric (also known as a taffeta) to reinforce the polyphtalamide matrix was made since this type of fabric is known for its good properties (good stability and low deformability during the manufacturing process). In addition, the plain weave structure gives the reinforcement substantially similar mechanical properties in both weft and warp directions giving rise to a relatively isotropic behavior. The weight fraction of Glass Fibers (GF) in the composite parts was verified by weighing 3 different specimens (5 cm x 5 cm) before and after incineration at 500 °C in air environment during at least 2 hours. The experimental volume and weight fractions of GF were thus measured to be around 30% and 60% respectively. It's useful to note that the glass fabric used in this study contained a special fiber sizing formulation based on PA and its copolymers (Hydrosize PA846) to make it resistant at high temperature (< 350 °C). This sizing is particularly suitable for high performance glass fiber applications [36, 37]. Finally, the GF fabrics were dried for 12 hours in a vacuum oven at 100 °C before being placed in the mold.

2.3 Preparation of composites

The installation employed was chosen to match the specifications and constraints imposed by the selected chemistry. It consisted of a bi-component machine composed of a twin-screw extruder, connected to a closed mold. The prepolymer/CA systems with an optimal stoichiometric ratio were prepared thanks to the developed hybrid system (extrusion - injection) detailed below. The mixing

between the prepolymer and chain extender agent was carried out in a co-rotating twin screw extruder (Haake Polylab System, Rheocord RC400P, Thermo Scientific, Karlsruhe, Germany) with a screw diameter of 16 mm and an L/D ratio of 25:1. The parameters of extrusion were the following: screw speed of 800 rpm, temperature profile of 270, 275, 280, 280 and 280°C from the feed zone to the die. The screw profile was designed to be adapted for the extrusion of low-viscosity systems. The prepolymer powder was fed into the twin-screw extruder using a Brabender gravimetric feeder (DDW-P2-MT-1, Brabender, Duisburg, Germany). A high melting temperature of the prepolymer and an efficient mixing step is needed to unsure a total homogeneity between the chain-extender and the prepolymer before filling. Thus, a mixing head was specially designed and fitted to an area of the extruder in order to spray at high pressure the 'CA' onto the molten prepolymer. This mixing head was fed by a metering pump to control the amount of 'CA' to be sprayed inside the extruder (and ensure stoichiometric control), (Figure 3). The last zones of the extruder, the transfer station and the mold were maintained at a constant temperature of 280 °C, 290 °C or 300 °C. The set point temperature of the metering pump spraying the 'CA' into the extruder was set at 160 °C, i.e., just above the melting point of CA. Once the extruder and the mold were stabilized at the set point temperatures, the prepolymer and the chain extender were simultaneously introduced at a predetermined flow rate to ensure optimal stoichiometric conditions. Finally, a thermoregulated transfer station was conceived to connect the extruder to the mold with the homogeneous flow velocity profile through a sheet of fluid in the form of a fish tail. Thus, for a flow rate of 1.3 Kg/h, and in view of the geometry of the system (tube, then plate), the apparent shear rate was estimated to respectively $70s^{-1}$ and $10s^{-1}$ in the injection channel and at the entrance of the mold.

For the studied filling flow rate, the measured pressure at the injection part beyond the mold doesn't exceed 3 bar. It was measured by pressure transducers in the entrance zone of the mold. To help to avoid voids at the final parts, the filling could be assisted by vacuum through the event connected to a special pump. Since the viscosity of the medium was too low up to mixing zone (i.e. high speed), the time needed for the injection to produce the composite part was controlled to be as short as possible. With the chosen flow rate, the mold which it displays a small volume is completely filled beyond 20 s in which the viscosity is less than 10 Pa.s. After filling the cavity of the mold, and after a few seconds of evacuation through the vent, the extruder was stopped and the mold was isothermally maintained for 2 minutes.

The cooling cycle was then quickly triggered by the thermoregulator to reach an indicated temperature of the heat transfer fluid of 100 °C. When adding the phases of demolding and cooling, the total cycle time to obtain the composite part did not exceed could reach 4-5 min in maximum.

Figure 3. *Photo of the used mixing head coupled to the metering pump for the injection of the chain extender agent onto the molten prepolymer in the extruder.*

2.4 Process installation used to monitor the hybrid T-ERTM process

A special instrumented mold was developed for this study with temperature and pressure transducers. It had a rectangular cavity with the following characteristics: H: 3 mm, L: 400 mm, W: 12 mm. No demolding agent was used before filling. Furthermore, no difficulty was observed to remove the composites parts during the demolding step (Figure 4).

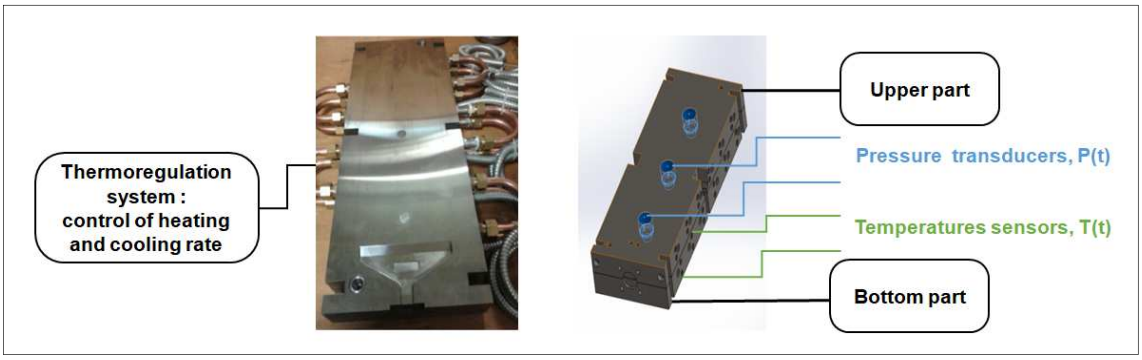

***Figure 4**. Design (left) and realization (right) of the instrumented and thermoregulated RTM mold.*

The mold was cooled by an independent oil circulation making it possible to vary the cooling rate. The mold was pre-heated one hour before and the system was made inert by N_2 gas. The computer acquisition system has been developed internally and allowed the collection of all the data from the pressure, temperature and dielectric sensors (Figure 5). These sensors are resistant to high temperatures and had a fast acquisition capacity (2 scans / sec). In addition to determining the pressure and temperature profiles throughout the mold cavity, the ultimate objective was to correlate the effective viscosity of the formulation with ionic conductivities obtained by in-situ metrology.

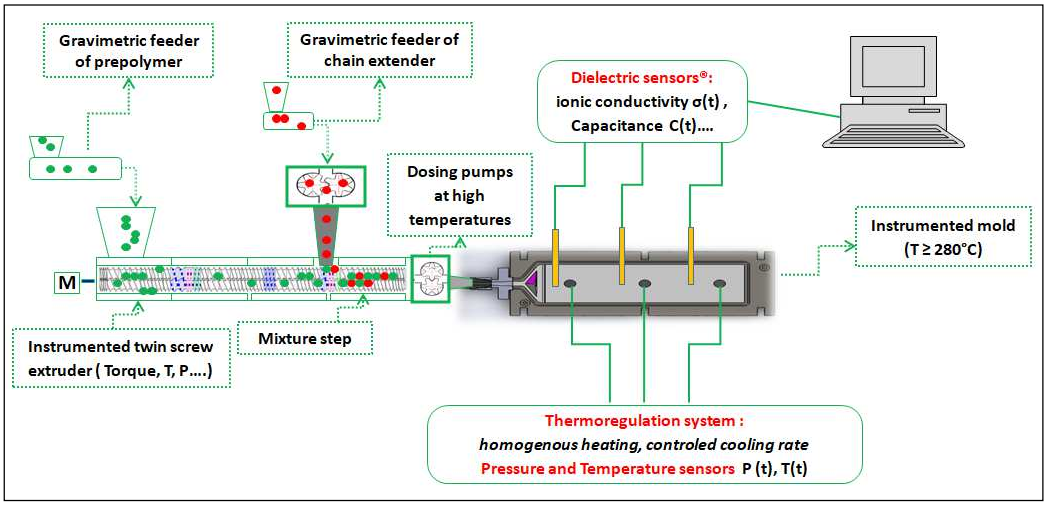

***Figure 5**. Thermoplastic extrusion resin transfer molding (hybrid HT-ERTM process) developed in this work. Instrumented mold for process monitoring [23].*

2.5 Characterization of PPA and its composites

2.5.1 In-situ/online monitoring of the reaction in the mold

Dielectric spectroscopy (DRS) was applied for in-situ monitoring of the process and the measurements were conducted using a spectrometer (20 Hz to 200000 Hz) coupled to a Varicon sensor. A method for interfacing the instrument with the sample as well as with the procedures used

for data analysis was developed. Data were collected especially at 20 Hz in order to capture the ionic conductivity and decouple it from dipolar relaxation. The system was programmed to store successive sets of data, rendering possible the real-time examination of the reaction process. The reaction process was depicted by a decrease in permittivity as well as by a drop in conductivity. The decrease of the specific conductivity resulted from a modification of the conductive paths and the increased viscosity. An experimental approach was proposed to follow the reaction process by dielectric measurements. The ultimate goal of this approach is to propose a correlation on the one hand between ionic conductivity of the system evaluated by in-situ measurements and on the other hand the viscosity of the medium determined by modeling at short times. This was in view of a better control of the process and in particular the impregnation step.
DRS is extremely susceptible to small changes in material properties, such as the segmental motion, molecular relaxation, chemical reactions and dipole changes. Therefore, DRS can be a sensitive probe to detect local motions that involve chemical reactions, in terms of changes in ionic mobility. This technique is a good complement to rheological measurements by identifying the transitions from the electrical properties of the materials. The complex dielectric constant with relative permittivity and loss factor were determined directly. Their mathematical formalisms are given in the appendix (A).

2.5.2 Ex-situ monitoring of T-ERTM reactive processing

2.5.2.1 Small Amplitude Oscillatory Shear (SAOS) in coupling with FTIR

To validate the metrology used for in-situ measurements and in order to find a correlation between the temporal variations of the ionic conductivity in dielectrometry with those of viscosity, ex-situ measurements using chemo-rheology coupled to the fast scan FTIR spectroscopy (evolution of the area of peak absorbance of esteramide reactive groups during the reaction, located between 980-930 cm^{-1}) have been performed. The change in viscoelastic properties with time and temperature were therefore recorded at the same time as an absorbance/transmittance spectrum in the confined heated chamber geometry. To achieve this goal, FTIR-ATR spectroscopy was carried out on molten samples at the same time as rheological tests using a Rheonaut ATR sampling module (Nicolet instruments) coupled to a thermo scientific HAAKE MARS 3 rheometer. Spectra were recorded at an average rate of 2 scans per second in the range 4000-700cm^{-1} with a resolution of 4 cm^{-1}, within a temperature range of 280°C to 300°C. The flow rate of nitrogen was set to 10 ml/min by a flow meter. Nitrogen purging (convection) was maintained throughout the experiments.
It is worth mentioning that for accuracy of measurements, dynamic viscosity modulus given respectively by RheoMars (SAOS/FTIR coupling with cone plate geometry) and DHR rheometer (from SAOS with parallel-plate geometry) were compared. They showed to be very close and validate the specific confined geometry developed for SAOS decoupled measurements.

2.5.*2.2* Small Amplitude Oscillatory Shear (SAOS)

SAOS measurements of PPA/CA formulations and their virgin constituents were determined in dynamic mode with a shear-stress controlled Discovery Hybrid Rheometer (DHR-2) from TA Instruments. The rheokinetic study was performed by monitoring the viscoelastic parameters in dynamic time sweep test (from 280 °C to 300 °C) and at an angular frequency of 1 rad/s. The studies were conducted in the linear viscoelastic regime previously established for each experiment. Before preparing the samples for the rheological measurements, the reactive systems and their virgin constituents were dried under vacuum for 12 hours at 80 °C in order to eliminate any trace of residual moisture. For only SAOS measurements, the sample in the form of compressed powder was placed in a cell contained in a confined controlled environment especially designed and adapted to the low viscosity of the starting systems. Experiments were performed in a plate-plate geometry using a plate diameter of 25 mm and a gap of ~ 1 mm. An axial force adjustment program was put in place to avoid any influence on the accuracy of measurements.

2.5.3 Measurements of torque using a micro-rheology compounder

5 g of PPA/CA blends were prepared using a twin-screw micro-compounder (Haake, Minilab II from Thermo-Scientific, Germany). For each formulation, the mixing torque (in N.m) was monitored as a function of time to follow and predict the end of the reaction. All the PPA/CA specimens were produced under an inert atmosphere thanks to a stream of nitrogen.
To mix the two constituents in a homogeneous manner, the chain extender was added vertically using a piston with a funnel to the top of the screws where the PPA prepolymer was in its molten state. The machine was purged and cleaned before each test. The reactive system could be circulated through a channel in order to pass through the compounder several times, making it possible to control the residence time of the reaction. The materials were blended in a temperature range from 280 to 300 °C for a variable duration of 1 to 20 min at a constant rotational speed of 50 RPM.

2.5.5 DSC measurements

Differential scanning calorimetry (DSC) measurements were performed on a Q20 (TA instruments, USA) calibrated with indium standards. A Rapid Cooling System (RCS) with a nitrogen flow of 50 mL min^{-1} was used down to -80°C. Samples of 5–10 mg were sealed in non-hermetic aluminum pans and were tested in the temperature range from ambient to 300 °C at a rate of 10 °C min^{-1}.

2.5.6 Size exclusion chromatography

Characterization by size exclusion chromatography (SEC) was used to measure the molar mass distribution of the reacted polyphtalamide samples at different experimental conditions (time, temperature). The analyses were performed with hexafluoroisopropanol (HFIP) as the eluent. The detection was carried out using an Agilent 1100 refractive index detector and the column was calibrated using a set of poly (methyl methacrylate) standards. The sample solutions in HFIP were prepared at 25 °C 1 day prior to the measurement in order to obtain good solubility. The PPA concentration was 1 g/L. Sample solutions were filtered through 10µm porous PTFE membranes prior to the measurements. SEC analyses made it possible to determine the molar mass characteristics (number and weight average data, $\overline{M_n}$ and $\overline{M_w}$, respectively) and the polydispersity index$I_p = \frac{\overline{M_w}}{\overline{M_n}}$. The molar mass obtained are expressed as PMMA equivalents.

2.5.7 Size titration of carboxylic acid end groups

The reaction between the chain extender "CA" and the PPA prepolymer is a polyaddition resulting in the consumption of the terminal carboxylic acid groups 'COOH' by the oxazoline functions. The carboxylic acid end-group content was determined using the Waltz–Taylor method [38]. The sample (1 g) was dissolved in 50 mL of a trifluoroethanol/chloroform mixture. Titration of this solution was carried out using a Mettler Toledo automatic titrator with 0.05 N of tetrabutylammonium hydroxide in an acetic acid solution.

2.5.8 Microscopic observations

To qualitatively investigate the fiber-matrix interface and to observe the quality of impregnation in the composite specimens, optical microscopy was carried out at different surface zones of composites using a stereomicroscope STEMI SV 6 from Zeiss at 3.2 magnifications with KL 2500 LCD lighting from Schott. For the investigation of the wetting between the fiber and matrix, Scanning electron microscopy (SEM) was performed. It was carried out in a HITACHI S-3500 N using an applied tension of 20 kV. To avoid damaging the morphological structure of composite parts before SEM observations, the composites samples were not cryogenically fractured. The observed layers have been delaminated from the composites specimens at the end of the mechanical tests, thus allowing to probe the quality of impregnation inter and intra-wicks.

2.5.9 Dynamic Mechanical Analysis (DMA)

DMA tests were performed using a Q800 DMA from TA instrument on samples with a rectangular shape (60 mm x 10 mm x 3 mm). The experiments were carried out according to the DIN EN ISO 6721 standard in flexural mode using a three-point bending clamp, with a constant heating rate of 3°C/min, a frequency of 1 Hz and a strain amplitude of 0.1%. Dynamic temperature weep tests were conducted in the temperature ranged from 25 to 250 °C. The rectangular samples were cut from the plates obtained from the forming parts (in the flow direction) and were dried for 12 hours at 100 °C before the measurements.

2.5.10 Flexural tests

Three-point flexural tests of all the composites and neat matrix were carried out on a Shimadzu AG-X tester (Japan) equipped with Trapezium® software with a 5-kN loading cell. The bending test speed was 2 mm min^{-1} and the span to sample thickness ratio was equal to 16. The flexural test was conducted according to NF EN ISO 14125 under the standard laboratory atmosphere with a temperature of 23 °C ± 1 °C and a relative humidity of 50% ± 5%. A minimum of five flexural specimens were tested along the flow direction for each reported value.

3. Results and discussion

3.1 Thermal properties of unreinforced PPA/CA samples

Figure 6 shows a typical DSC temperature scan of neat PPA, neat CA and a PPA/CA bi-component system carried out at a heating rate of 10 °C/min. It was clearly observed that the bi-component system before reaction (red curve) presented a glass transition temperature around 100°C corresponding to the Tg of the polyphtalamide (PPA) prepolymer, a melting temperature T_m of the 'CA' around 150°C and a melting temperature of PPA around 270 °C. After the reaction, a shift in the glass transition was noticed and Tg reached a value of 115 °C which signifies the presence of more cohesive PPA chains. This shift in the glass transition mirrors the extension chain reaction. It should be noted that the significant increase in Tg observed between the first and the second heating cycles confirmed that the reaction was very fast. Consequently, the use of DSC to probe polymerization kinetics at of reaction was very difficult.
During the first scan, a baseline difference was observed. In fact, the bit change of the baseline due to the chain extension reaction took place simultaneously with the endothermic peak corresponding to the melting of the of the polyphtalamide crystalline part. Indeed, it was difficult to separate these two phenomena and similar results were reported in the case of in-situ polymerized cyclic butylene terephthalate or caprolactam [19, 23]. However, the reaction is shown to not have a high exothermic energy. It presents a very low exothermal behavior as we have demonstrated by non anisothermal DSC investigations and kinetic modelling [36]. For the clarity purpose, these results will not be shown in this paper. Hence, our chosen systems seems to not affect the interfacial bonding between polymer matrix and fibers in the contrary to other reactive thermoset systems [39].
Once completely reacted, a change in the melting peak was also observed. In fact, the chain extension reaction was found to lead to profound changes in the crystallization mechanism of PPA. This was manifested by the presence of a double melting peak, which may be explained by the presence of different crystal sizes. Chain extension reaction permits to form PPA long chains with different chain distribution as was demonstrated by SEC measurements (section 3.2.3). Thus, it allows them to crystallize differently. With a second and a third heating, the observed double peak is reproducible confirming two kinds of crystalline melting (i.e. thermodynamically different). Meanwhile, this double peak is shifted to high melt temperature with increasing reaction time. Furthermore, two melting peaks were observed which suggests the presence of different crystal sizes as reported in other literature data [40]. This hypothesis has not been validated during this

work and it will be a subject of a featuring work including X-ray and Polarized Optical Microscopy investigations.

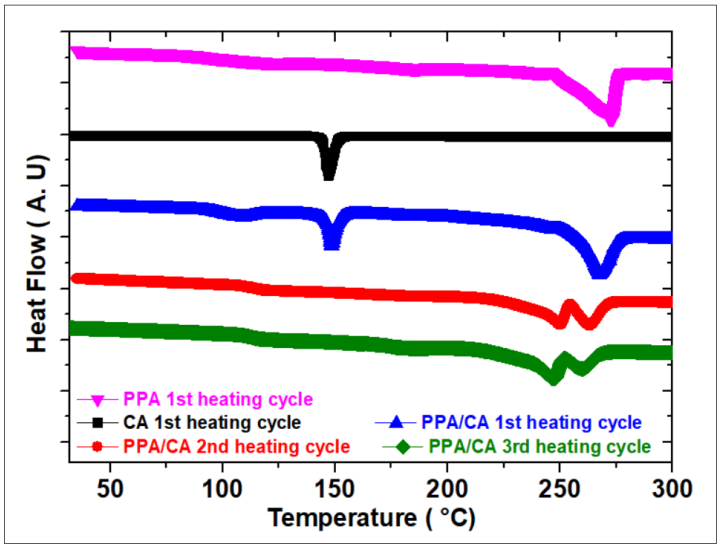

Figure 6: DSC curve at a heating rate at 10°C/min for neat PPA, CA and the PPA/CA system. Comparison of 1st, 2nd and 3rd heating scans.

The same reactive PPA/CA system was maintained isothermally at 280 °C at different reaction times (Figure 7). Subsequently, the evolution of Tg and Tm with the time of the reaction was measured by DSC and the results are summarized in Table 2. The glass transition temperature was found to increase gradually over the reaction time. Surprisingly, the increase in Tg was not significant at short times (2 and 4 minutes). As the reaction proceeded, the Tg continued to increase with increasing conversion, since a high conversion led to long-chain polymers and hence to a high molecular weight could be reached [41]. The shift in the glass transition with increasing reaction time is assigned to the high conversion of the produced polyphtalamides, and hence to higher molecular weights.

Beyond the Tg zone, we observed the presence of a first endothermic peak located around 187 °C, believed to correspond to the melting of the polyundancanamide part (polycondensation of the undecanamide present in the initial formulation of the prepolymer). One could then observe the presence of two endothermic peaks corresponding to the melting of different-sized crystals of the formed polymer. Indeed, thicker and stable crystals exhibit a higher melting point than their finer counterparts. On the other hand, the melting temperature also increased with the evolution of reaction time. The increased conversion may lead to the formation of well-ordered crystals with strong inter-chain interactions. Since the melting point reflects the chain motion in the crystals, it was logical that the melting temperature was higher in the case of high molecular weight samples [42]. A further discussion of this subject is given in section 3.2.3.

***Table 2**: Values of the glass transition temperature (Tg), melting point $T_{m,1}$ (first peak), melting point $T_{m,2}$ (second peak), at different reaction times. The reactive bi-component system corresponded to a temperature of 280 ° C.*

Reaction time	0	2	4	6	10	20
Tg (°C)	100	102	104	107	110	115
$T_{m,1}$ (°C)	270	239	242	242	247	247
$T_{m,2}$ (°C)		253	256	254	260	260

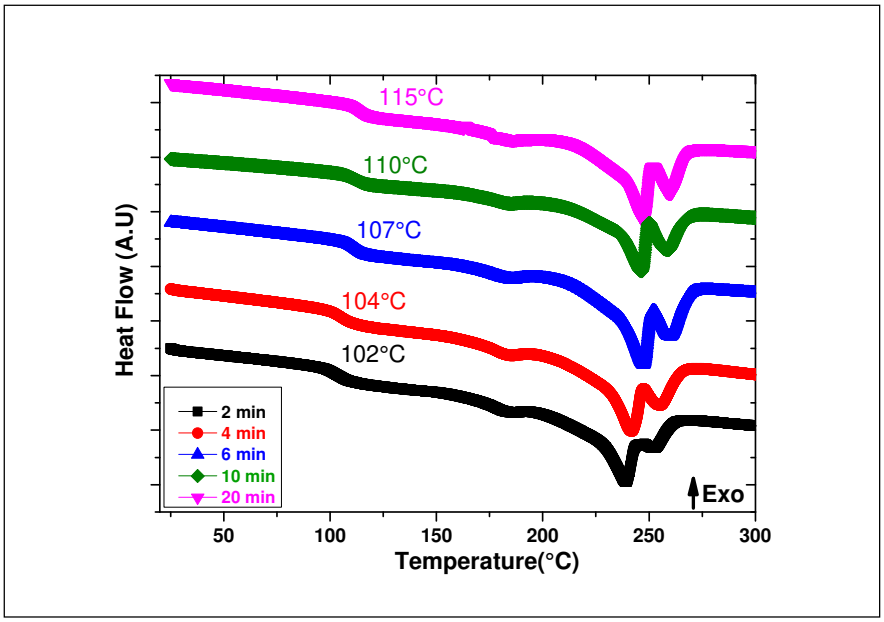

***Figure 7**: Comparison of DSC thermograms performed at 10°C.min^{-1} on PPA/CA systems at 280 ° C following different reaction times (2,4,6,10 and 20 minutes).*

3.2 Chemo-rheological study

3.2.1 Torque measurements in a Minilab micro-rheology compounder

The occurrence of chemical interactions between the prepolymer and the chain extender in the molten state were qualitatively assessed by recording the evolution of the torque as a function of time using the micro-rheology compounder. In these experiments, the PPA prepolymer was introduced first after which the 'CA' was added at t=1min in an appropriate amount to achieve optimal stoichiometric conditions. The time required for the completion of the chain extension reaction was that when the torque reached its maximum value. Figure 8 shows the torque profile recorded at different studied temperatures. The introduction of the 'CA' into the initial prepolymer melt caused marked changes in the torque of the PPA/CA system. This rapid raise of the torque in the molten state was the result of the increase in melt viscosity of the formed PPA by the chain extension reaction between the oxazoline functions of the 'CA' agent and the carboxyl terminal groups of the PPA (see the proposed mechanism in the section 2 mentioned above).
However, as previously mentioned, a secondary reaction of branching can take place. From Figure 8, it was clear that the shape of the torque profile depended on the temperature before reaching a plateau. An increase in reaction temperature reduced the time needed to achieve the end of the reaction and the maximum torque value. It was here demonstrated that this time decreased dramatically with increasing temperature. The chain extension reaction was completed after approx. 15 min at 280°C and approx. 7 min at 300°C. Nonetheless, a significant torque drop occurred at long times when the reaction temperatures were 290 °C and 300 °C, but not at 280 °C.

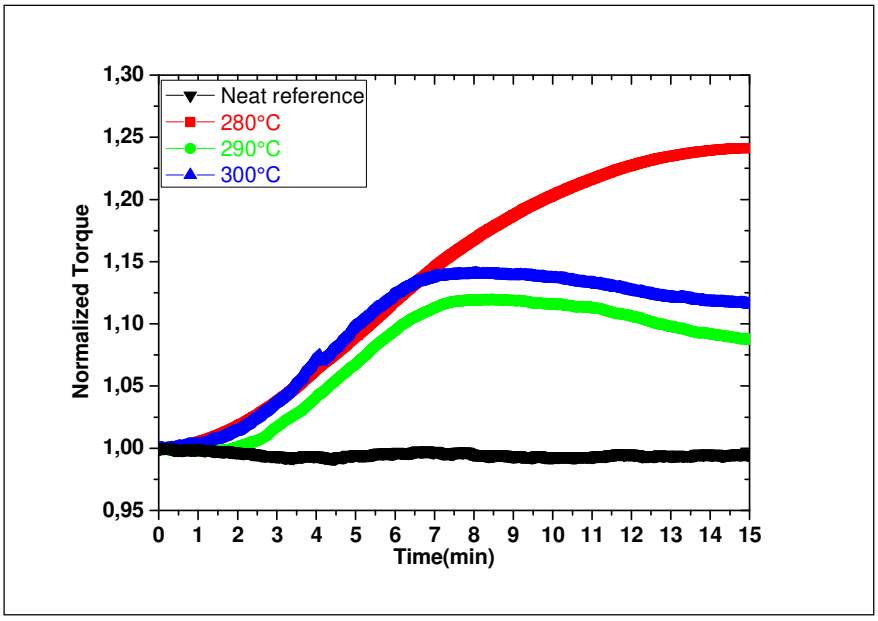

***Figure 8**. The evolution of the normalized melt torque [C(t)/C(t=0)] as a function of the reaction time at different reaction temperatures.*

PPA/CA samples taken at 2 and 15 minutes of reaction at 280 °C were immersed in HFIP for dissolution.

From Figure 9b, we can clearly observe some non-soluble parts of the polymer after 15 minutes of reaction, indicating the formation of a network (secondary reaction branching), similar to what we can obtain at high stoichiometry [27].

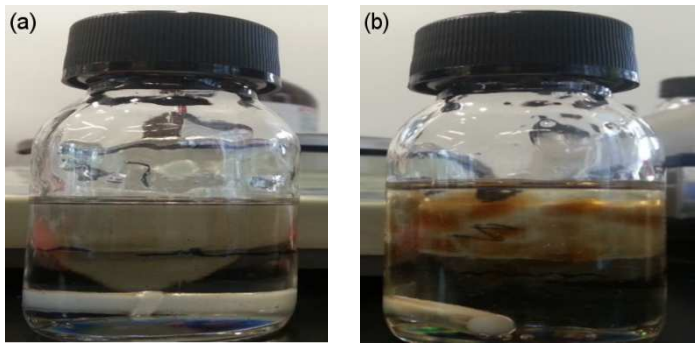

***Figure 9**. Example of the solubility of the PPA/CA bi-component system (a) after 2 minutes, and (b) after 15 minutes of reaction at T=280°C.*

It is worth mentioning that the results shown in Figure 8 cannot determine with accuracy the reaction kinetics. In fact, the fairly rapid increase in torque following the addition of the CA agent into the PPA cannot be clearly probed from a kinetic point of view (the time needed to start and end the reaction). This result provides qualitative information indicating that the reaction that occurred in the PPA/CA systems was drastically influenced by changes in temperature and reaction time.

3.2.2 Influence of temperature and reaction times: chemo-rheological study

The polymerization process can also be followed by dynamic rheological measurements under isothermal conditions, since the chain extension reaction is directly related to the change in viscoelastic properties, such as storage modulus (G'), loss modulus (G") and viscosity (η) of the materials. The influence of the polymerization temperature on the viscosity profile is presented in Figure 10 where viscosity spectra are plotted as a function of time comparing the PPA/CA systems with neat PPA prepolymer. It is worth mentioning that the time needed to stabilize the temperature for isothermal measurements was optimized to 1.5 min. For accuracy and confidence, the results

were recorded after isotherms of two minutes. Making the situation more complex, it was found that the viscosity that was initially below 3 Pa.s rose very rapidly during the first two minutes required to reach and stabilize the temperature. Indeed, in 2 min, the viscosity reached 180 Pa.s and 73 Pa.s at 280 °C and 300 °C, respectively. The results show once again that the beginning of the reaction was very fast and that the reaction was almost instantaneous between the PPA and CA making rheo-kinetic studies at short times very difficult. Thus, rheometry showed its limit for the present system especially at first time of reaction. We also note a decrease in the viscosity when the reaction time reached 10 min at 300 °C probably due to the thermal degradation of the polymer at high temperatures.

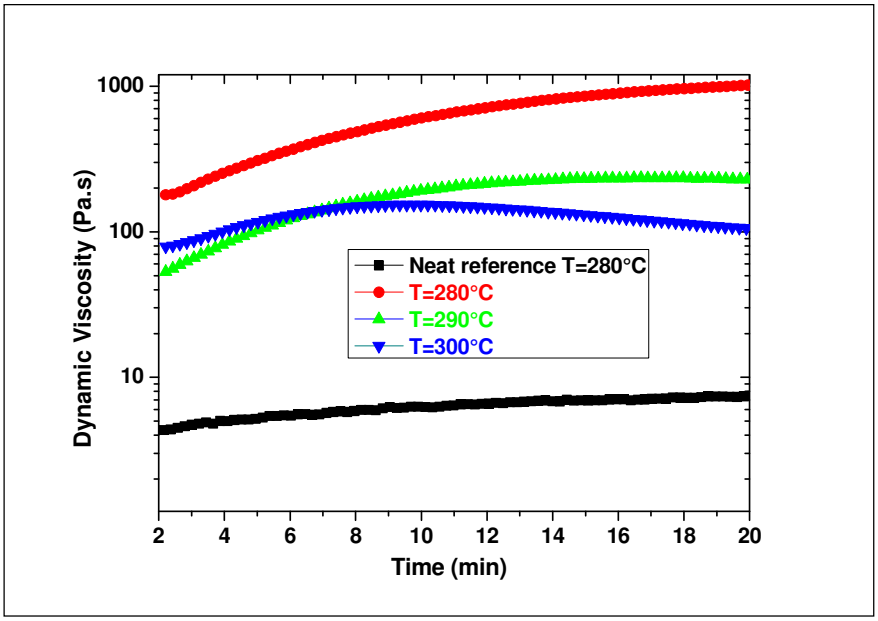

***Figure 10**. The evolution of the dynamic viscosity modulus at an angular frequency of 1 rad/s for neat PPA and PPA/CA systems at 280°C, 290 °C and 300°C.*

3.2.3 The effect of the reaction time on the molar mass properties

The molar mass properties of the obtained PPA were recorded at different reaction times (at 280 °C). They are illustrated in Figure 11. It can be seen that the values of $\bar{M}_n$ and $\bar{M}_w$ increased significantly at less than 5 minutes of reaction. Furthermore, the polydispersity indices continued to increase significantly indicating a high sensitivity of the weight average molecular weight ($\bar{M}_w$) to structural evolutions. The molar mass increased sharply to reach values around 260 Kg/mol. As a result, the distribution of macromolecular chains became broader at long times. In comparison to other polyamides systems, the PDI stabilized after 15 min of reaction at an index of 25. These results confirmed that some chain branching could influence those properties rather than chain extension. Hence, the first mechanism was the chain extension between the ends of COOH chains and oxazoline. The secondary mechanism consisted of branching of the macromolecular structure at temperatures above 280 °C and at long times manifested itself by a significant increase in polydispersity index.

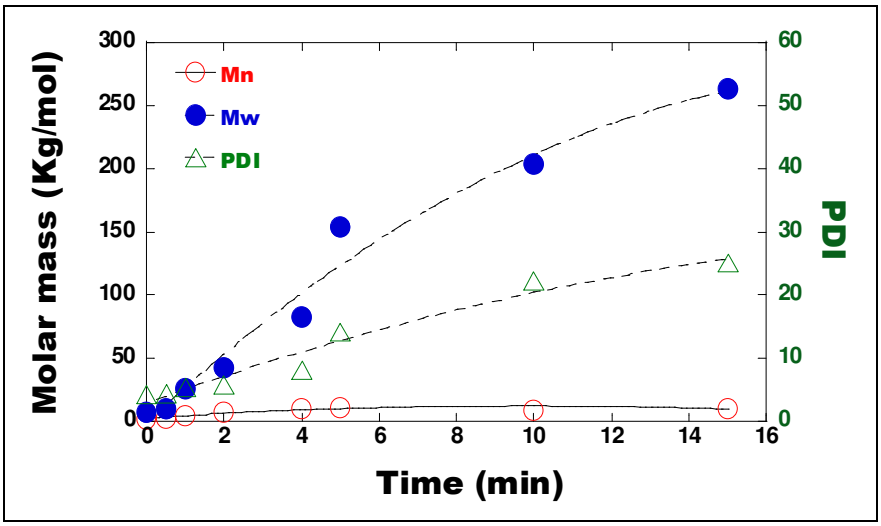

***Figure 11**. Evolution of the weight average molecular weight ($\bar{M}_w$), the number average molecular weight ($\bar{M}_n$) and the polydispersity index (PDI) as a function of time for PPA/CA systems at 280 °C.*

3.4 Titration analysis

Reaction kinetics were also studied using the titration method. The acid content of the PPA prepolymer before and after processing in the micro-rheology compounder was determined by titration of acid end groups. The apparent conversion of the polymerization was calculated using equation 6:

$$x = \frac{[C]_i - [C]_t}{[C]_i} \qquad \text{(Eq. 6)}$$

Where (x) is the conversion rate, $[C]_i$ the initial concentration and $[C]_t$ the concentration at time t.

Figure 12 portrays the reaction conversion as a function of time at 280 °C. The results show that the beginning of the reaction was very fast and that the conversion reached 80% after two minutes without any significant changes in residual acid detected after 15min of polymerization. Since the reaction between PPA and CA was so fast, it was extremely difficult to track the reaction kinetics at short times by the titration method.

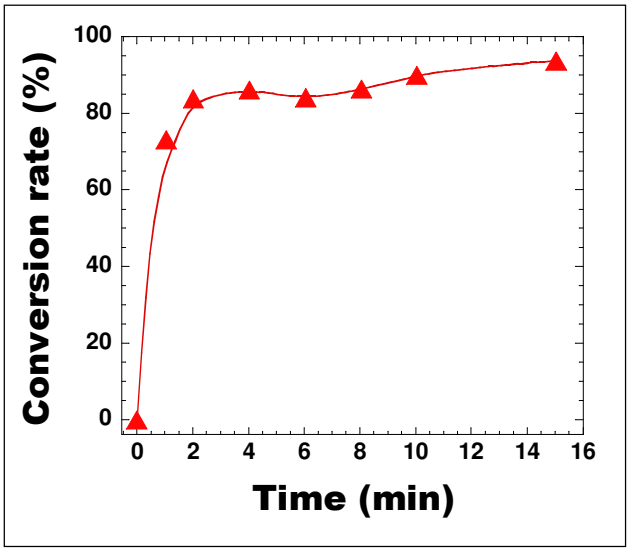

***Figure 12**. Conversion rate as a function of the reaction time of PPA/CA system at 280°C.*

3.5 Coupling Fourier transform infrared spectroscopy to rheology

The monitoring of the polymerization reaction at short times by conventional techniques (rheometry, DSC and titrations) was inconclusive. To overcome these constraints, an Infrared Rheology Coupling System was chosen. This system had the advantage of coupling the kinetic study of the reaction via infrared monitoring to the evolution of the dynamic viscosity modulus. To attain this objective, both theory and experiments were performed to establish a rheo-kinetic model allowing us to quantify the viscosity, especially at short times, and also in order to predict the processing window.

The peak area at (980-930 cm^{-1}) was used for the quantitative analysis of the reaction rate. The abovementioned peak area was assigned to esteramide [43]. At 0 min (neat prepolymer), the band at 980 cm^{-1}, characteristic of the esteramide group, was completely absent, then started to appear as the reaction progressed. In fact, an esteramide is the result of a reaction between oxazoline and a carboxyl group as mentioned when discussing the mechanism of the chain extension reaction cited above. These bonds were monitored independently during the polymerization to follow the reaction kinetics. The absorption intensities were normalized by the hydrogen bonds at 2900 cm^{-1} for the neat prepolymer and were used as a reference. Figure 13 shows a plot of the amide region (980-930 cm^{-1}) as a function of time. The extent of reaction with time was determined from the evolution of the amide area (peak area 980 cm^{-1}).

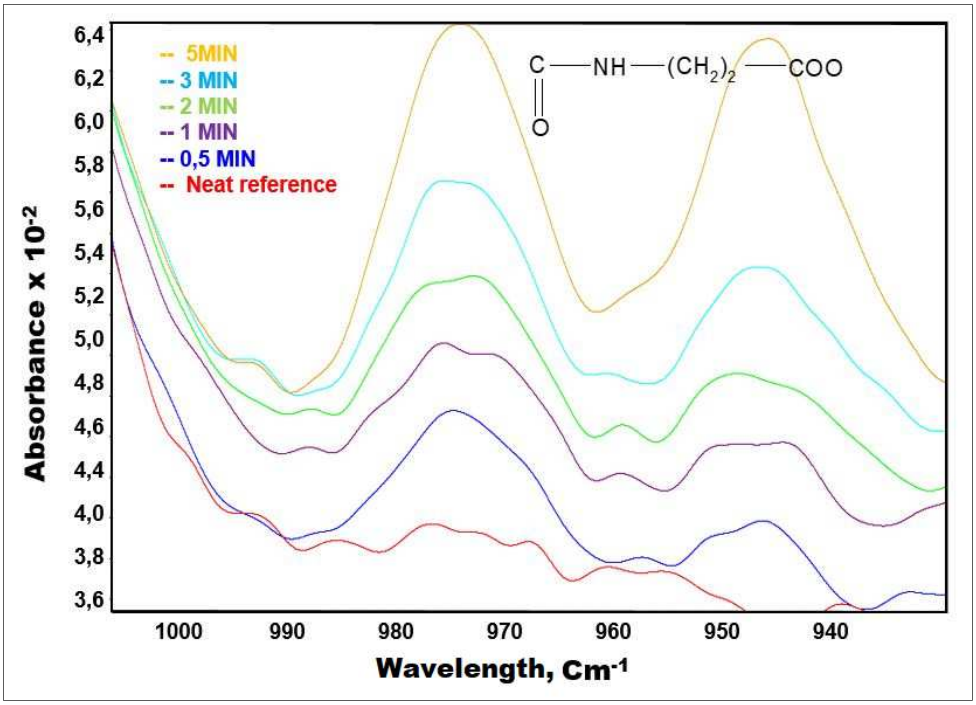

***Figure 13**. In-situ FTIR spectra during the reaction of PPA with CA at 280°C in the zone of (980-930 cm^{-1}).*

The normalized fractional conversion from the FTIR absorption data was calculated based on equation (7):

$$p(t) = \frac{A(t_f) - A(t)}{A(t_f)} \qquad \text{(Eq. 7)}$$

Here, p is the fractional conversion, A(t) is the area of the peak during time, and $A(t_f)$ is the area of the peak at the end of the reaction. For each system, the area of the relevant band was measured taking into consideration slight variations in the baseline. Figure 15(a) highlights that the reaction seemed to be very fast and that a maximum was reached in less than 120 s.

To establish a rheokinetic model, we studied the kinetics of the reaction by in-situ FTIR as well as the increase in viscosity during the reaction. The adequate equation for the variations of the

viscosity was derived from the molecular weight dependence. It follows a simple law expressed in the following equation.

$$\eta(t) = A\ exp\left(\frac{E_a}{RT}\right)\ [\bar{M}_w(t)]^n \qquad \text{Eq. (8)}$$

where E_a is the activation energy, T the temperature in Kelvin and n an exponent that is adapted depending on whether $\bar{M}_w$ is lower than (or equal to) 1 or higher than critical entanglement molecular weight M_c (i.e., equal to 3.4). The $\bar{M}_w$ is expressed as a function of the reaction conversion p(t) [44]. This apparent reaction extent could be evaluated according to equation 7.

$$\bar{M}_w(t) = \bar{M}_w(t_0)\frac{1+r\ p(t)^2+\frac{4r}{1+r}p(t)}{1-r\ p(t)^2} \qquad \text{Eq. (9)}$$

$$\bar{M}_w(t_0) = \frac{\bar{M}_w(t_0)\ [PA]+\bar{M}_w(t_0)[PBO]}{2} \qquad \text{Eq. (10)}$$

$\bar{M}_w$ from equation 10 can be introduced in equation 9 in order to model the viscosity evolution. Subsequently, this viscosity evolution can be expressed as a function of time and conversion p according to:

$$\eta(t) = A\ \exp\left(\frac{E_a}{RT}\right)\left[\left(\frac{\bar{M}_w(t_0)\ [PA]+\bar{M}_w(t_0)[PBO]}{2}\right)\left(\frac{1+r\ p(t)^2+\frac{4r}{1+r}\ p(t)}{1-r\ p(t)^2}\right)\right]^n \qquad \text{Eq. (11)}$$

At short times (t<90 sec), the logarithm of the zero shear viscosity was plotted as a function of $\log\ \bar{M}_w(t)$. It was found that the viscosity of the medium was proportional to the molar mass of formed macromolecules and a slope of 3.1 was obtained (Figure 14). This value of the slope indicated that we were in the presence of an entangled polymer even for very short reaction times (more than 10 s).

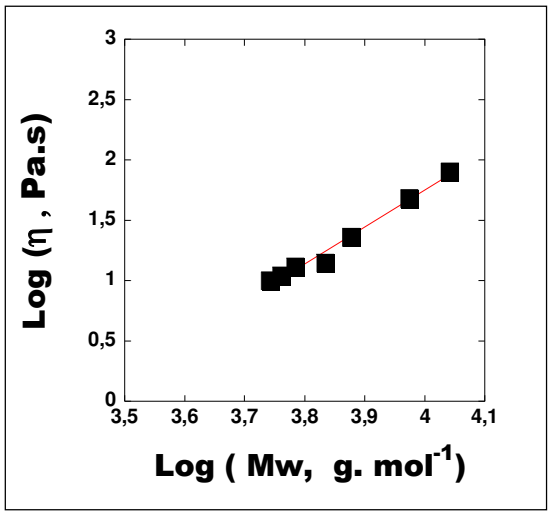

Figure 14. *Complex viscosity at 1 rad.s^{-1} as a function of the weight average molecular weight at 280 °C (logarithmic scale).*

Theoretical values from equation 11 were compared with the experimental measurements at reaction times over 2 min in the linear viscoelastic regime. Figure 15(b) shows the evolution of the complex viscosity as a function of time. The evolution of the apparent conversion followed that of the viscosity especially at long times. Figure 15(b) also displays how the experimental viscosity corresponds to that calculated from equation 11. The results show that the beginning of the reaction was very fast and that the conversion reached 80% and 70% at 280 °C and 300 °C, respectively, in 2 min. It was thus clearly demonstrated that the conversion as well as the viscosity increased drastically during the first 2 minutes. Figure 15(b) highlights a good agreement between the experimental data of the measured viscosity and its theoretical counterpart at 280 °C. The viscosity evolution as calculated by equation 11 fit the experimental data quite well in the first conversion

range. Moreover, the viscosity profile showed a signature of both chain extension and branching reactions especially at longer times. Indeed, a slight deviation from the experimental data was observed, especially after 10 minutes of reaction. However, the fit was less effective at 300 °C due to thermal degradation as we have demonstrated by molar masses measurements. These results also highlight a processing window for HT-ERTM processes including time for impregnation and to a maximum of reaction conversion. Thus, with these reactive system, the time frame for injection was consequently very short and making more complicate it's RTM adaptation. In sum, 2 minutes is a maximum holding time in the mold in order to reach 85% of conversion. Experimentally and with our chosen flow rate, the mold which it displays a small volume is completely filled beyond 20 s in which the viscosity is less than 10 Pa.s. The total cycle time before demolding could reach 4-5 min in maximum depending on the desired PPA molar masses.

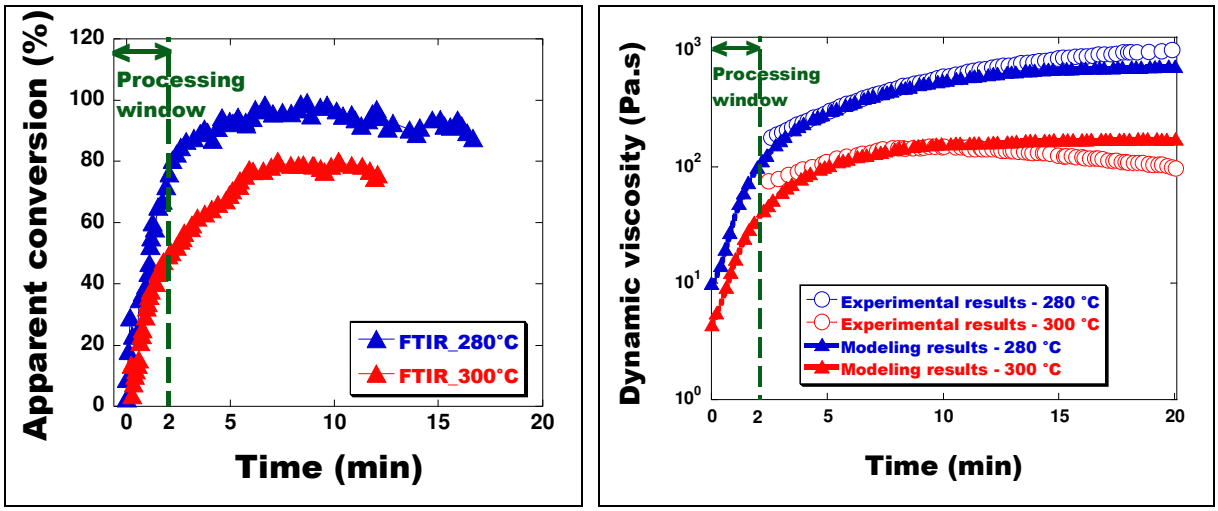

Figure 15. *(a) Evolution of the apparent normalized conversion for PPA/CA systems at 280 °C and 300 °C. (b) Comparison of theoretical viscosities predicted by equation 11 with the experimental values of the dynamic viscosity modulus versus time.*

3.6 In-situ monitoring of the reaction in the mold by dielectric measurements

The values of conductivity as a function of the reaction time were calculated from equation (5) and are represented in Figure 16(a). The dielectric properties of the system can be related to the material processing: (i) the increase in the PPA conductivity corresponds to the melting of the sample and stabilization of the temperature, (ii) the decrease in ionic conductivity after the peak maximum signified the start of the reaction, (iii) the conductivity plateau correlated well with the end of the reaction. Based on the validation of the procedure previously discussed in the experimental part of this paper, Figure 16(b) portrays the evolution of the reaction conversion with time for PPA/CA systems at 280 °C. It compares the conversion determined by FTIR spectra with that calculated by equation 5 from the in-situ dielectric measurement. Interestingly, the obtained evolution of apparent conversion recorded by the in-situ dielectric measurement during the process corroborated the ex-situ counterpart obtained by FTIR coupled to rheology and by titration as given in Figure 12.

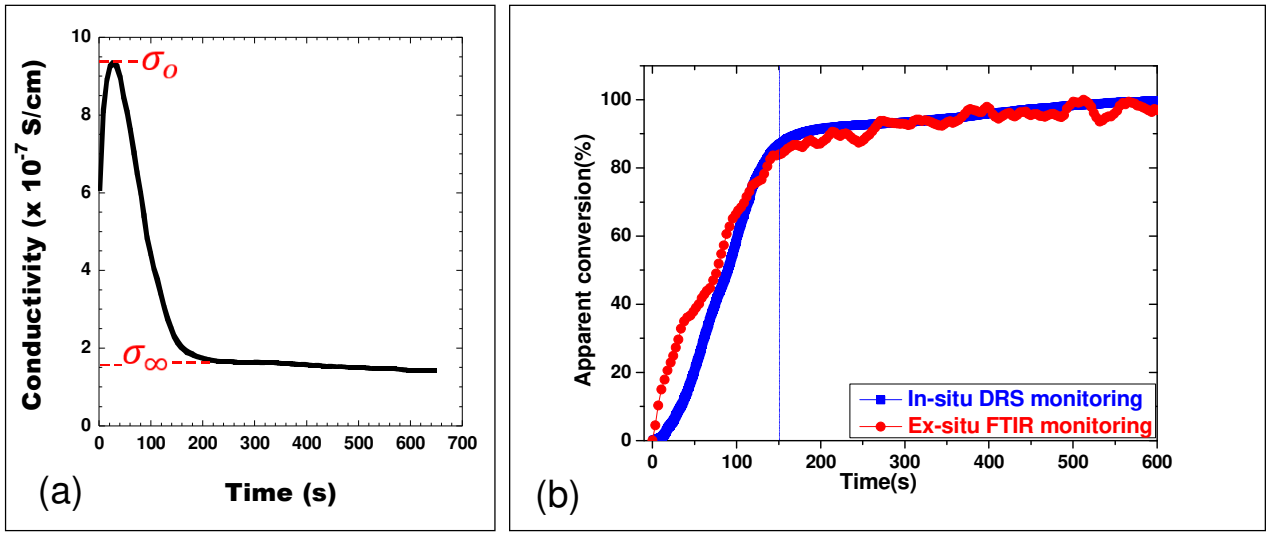

***Figure 16**. (a) Evolution of ionic conductivity as a function of time at T=280°C at a f = 20 Hz. (b) Evolution of the apparent conversion obtained from FTIR and dielectric spectroscopies as a function of time at 280°C.*

3.7 Correlation of dielectric in-situ monitoring with the evolution of viscosity during polymerization in the mold

Figure 17 shows the variations of the ionic conductivity measured in the mold by dielectrometry as a function of the modulus of the complex viscosity determined experimentally or by modeling at short times. The mold temperatures were either 280 °C, 290 °C or 300 °C. The obtained results demonstrated similarities between the variations of the ionic conductivity from dieletricometry with those of the viscosity as a function of time and temperature. According to the literature, Kranbuehl et al. [45] noticed that there was an inversely proportional relationship between viscosity and conductivity. Thus, the ionic conductivity decreases with increasing viscosity according to the so-called Stokes-Einstein law. In contrast, a deviation from the Stokes law is generally observed for non-homogeneous reactive media. Consequently, the so-called Walden's correlation can be given as follows [46]:

$\sigma(t)\,\eta(t)^m = \text{Const}$ with $m < 1$.

Here, (σ) is the ionic conductivity and (η) is the viscosity. Thus, our original contribution consists in taking into accounts the evolution of viscosity from in-situ/modeling approach.

Figure 17 shows that the higher the reaction temperature, the lower the amplitude of the ionic conductivity, thus resulting in a high reactivity of the PPA/CA system. Moreover, the presence of side reactions at long times leads to a loss of validity of the Walden equation since the fit is divergent in this zone [47].

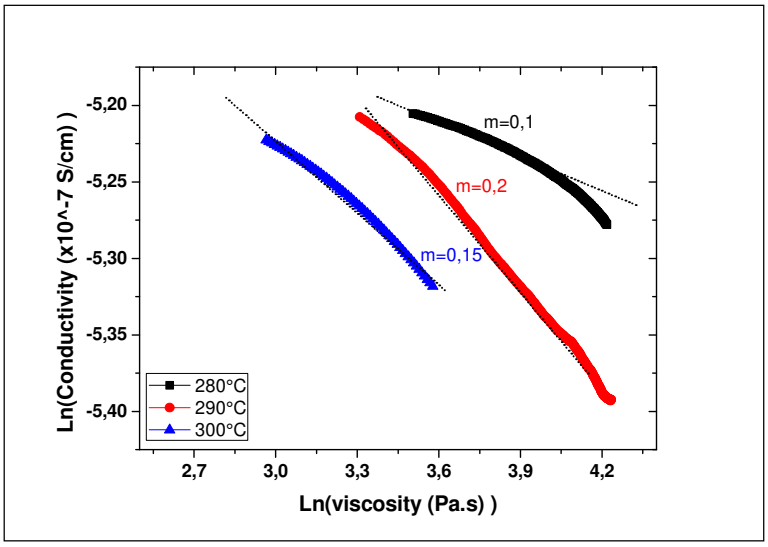

***Figure 17**: Logarithmic evolution of the ionic conductivity (measured at 20 Hz by in-situ dielectrometry in the mold) as a function of the complex viscosity modulus.*

3.8 Thermal properties of glass fiber-reinforced PPA/CA composites

Figure 18 compares DSC thermograms of three different zones of the composite part. Tables 3 and 4 summarize all the measured glass transition temperatures and melting enthalpies. It's important to note a certain reproducibility of measured Tg and melting enthalpies, regardless of where the sample was taken. One again, two melting peaks were observed which may have their origin in a double distribution of the crystalline phase. At a temperature close to 189 °C, the melting of polyundecanamide is clearly identified. These values of Tg, melting points and melting enthalpies corroborate those measured with unreinforced matrices as discussed earlier. This reflected some isotropy in properties in the different areas of the composite parts. To the best of our knowledge, the melting enthalpy of 100% crystalline PPA is not available in the literature, so the absolute degree of crystallinity for the PPA samples cannot be determined directly. Thus, it could be concluded that the chain extension reaction had indeed taken place homogeneously within the mold. In addition, the high values of Tg validated the efficiency of the used process and in particular the injection head and the screw profile.

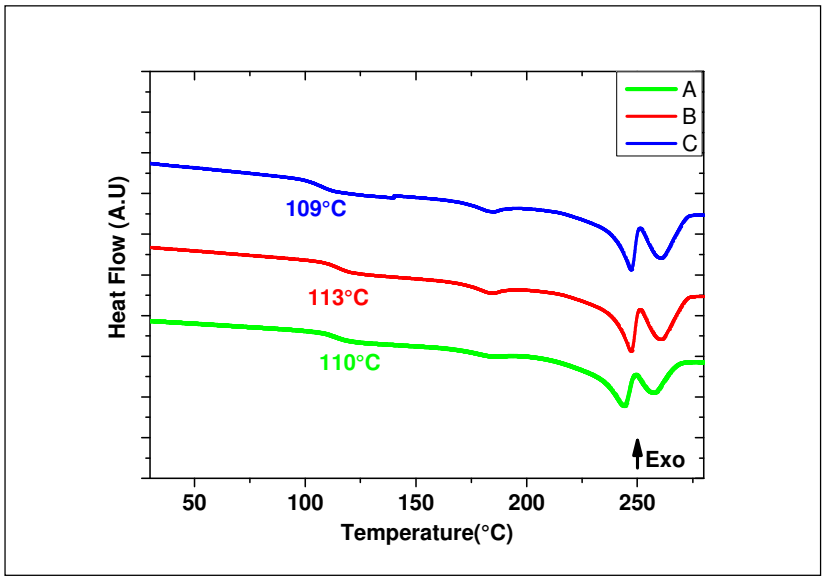

***Figure 18**: DSC scans (2st heating) of continuous glass fiber reinforced parts (PPA/CA bi-component systems injected at 280 ° C +60% by weight of glass fibers). Sampling at (A) the beginning of the flow, (B) in the middle area and (C) at the end of the flow.*

***Table 3**: Glass transition temperatures and melting points in the three areas of the composite parts.*

Sample n°	Tg (°C)	$T_{m,1}$ (°C)	$T_{m,2}$ (°C)
A	110	244	258
B	113	247	261
C	109	248	262

Table 4: The average melting enthalpy obtained using three different areas of the composite parts in comparison with pure matrix.

Sample n°	Melting Enthalpy (J/g)
Pure PPA matrix	59
Composite part	58

3.9 Microscopic observations of reactive GFRTC

The morphological observations at the micro scale on composites surfaces were conducted at different areas of the composite parts obtained at 280 °C as illustrated in Figure 19. It was found that a homogeneous wetting was obtained within and between the wicks. The glass fiber reinforcements were completely coated by the PPA matrix which seemed to be free from air bubbles. In addition, no lack of material was noticed indicating a good matrix/reinforcement impregnation. Therefore, the quality of the impregnation seemed to be the same regardless of the cutting area in the composite parts (a), (b) or (c).

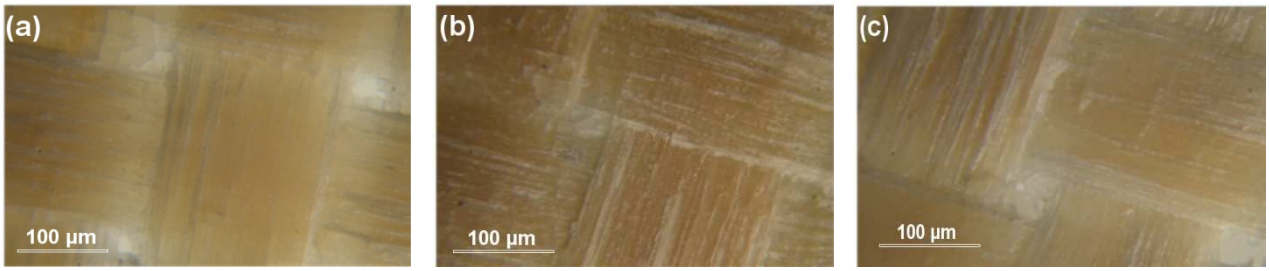

***Figure 19**. Optical microscopy observations of PPA/CA based composites. Sampling at (a) the beginning of the flow, (b) in the middle area and (c) at the end of the flow.*

To analyze the impregnation inter and intra-wicks, delaminated layers of PPA/CA composites have been analyzed using Scanning Electron Microscopy (SEM). As can be seen in Figure 20(a), a good wetting between fibers and matrix was observed. At high magnification, Figure 20(b) shows that a thorough wetting of the individual strands was achieved. Nevertheless, the micrographs indicate the presence of some holes and bubbles.

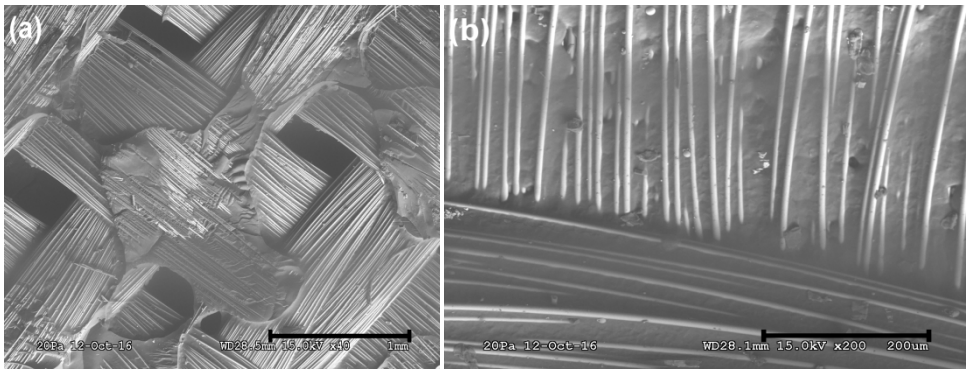

Figure 20. (a). Scanning electron microscopy (SEM) image of a cross section of PPA/CA composites. (b) SEM micrograph at high magnification.

3.10 Thermo-mechanical properties

The evolution of dynamic mechanical properties versus temperature of unreinforced and woven glass fabric reinforced composites was performed to investigate the glass transition temperature and the viscoelastic behavior at the solid state of the samples. Figure 20(a) depicts the storage modulus (E') and the damping factor (tan δ) as a function of temperature for PPA/CA specimens prepared at the optimal processing temperature, 280 °C. The peak of tan δ curve around 120 °C reflects the dynamic α-relaxation (glass transition). The storage modulus (E') in the glassy state was around 1.6 GPa. As soon as the Tα transition was approached, a decline in storage modulus occurred due to the enhanced chain mobility. However, as the melting of crystals approached, the elastic modulus (E') fell even more steeply. It should be mentioned that the storage modulus above the Tg ($E'_{rubbery}$) presented a non-flat rubbery plateau probably due to the alpha star transition ($T\alpha^*$) associated with the slippage between crystallites [48] and it was characterized by the appearance of a second peak in the region above the Tg located at about 183 °C. Moreover, some cold crystallization could appear.

The storage modulus (E') and damping factor (tan δ) of the glass fiber/polymer composites are presented in Figure 20(b). As can be seen, the composites showed significantly higher E' values than their unreinforced PPA/CA counterparts. Indeed, an increase in the elastic modulus of about 160% was observed ($E'_{composites}$ ~ 4.2 GPa). This augmentation of E' over the analyzed temperature range was attributed to the usual reinforcement effect caused by the fibers allowing a high degree of stress transfer at the interface. In contrast, the α relaxation temperature (Tα ~ 122 °C) remained almost unchanged. Nevertheless, the DMA results revealed a broadening of the tan δ peak with the incorporation of GF layers. This phenomenon should be assigned to the broadening of the spectrum of relaxation times due to the reduction of mobility by the anchoring of the chains in contact with the GF folds [49]. Indeed, the properties of the interphase usually differed from that of the bulk owing to different relaxation behaviors. Another effect of the reinforcement was the decrease in the height of the tan δ peak which could be assigned to a reduction of the mobility of the macromolecular chains in the vicinity of the glass fibers due to a good interfacial interaction between PPA matrix and GF folds which led to lower damping at the interface.

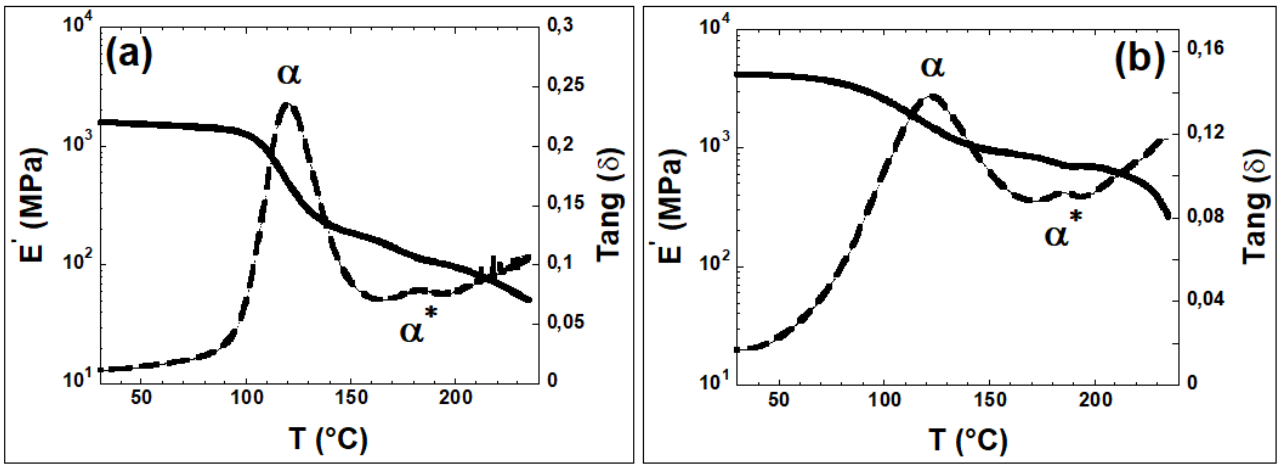

Figure 20. *Evolution of storage modulus and tan (δ) as a function of temperature for (a) a neat PPA matrix, and (b) glass fiber-reinforced PPA composites obtained at a reaction temperature of 280 °C.*

3.11 Flexural properties

The average values of the flexural modulus and the yield strength defined as the maximum bending stress, are given in Table **5**. It can be seen that the virgin polymer had a moderate yield stress of 33 MPa and featured a flexural modulus of 2.2 GPa. Furthermore, the composite parts presented a flexural modulus of the order of 16 GPA and a yield stress of the order of 120 MPa. Thus, the results obtained for the composite showed some adhesion and corroborated the adhesion properties revealed by the morphological studies. A Takayanagi model was used to predict the modulus values of the composite. The model considers the material as composed of two elements working in parallel. The first element consists of the entire fiber and part of the matrix, acting in series. The second element consists of the rest of the matrix [50]. The expression of the composite modulus using the Takayanagi model is:

$$E_c = E_m\left(1-\frac{V_f}{\Phi}\right)+\left(\frac{V_f E_m E_f}{E_m\Phi^2+(1-\Phi)\Phi E_f}\right) \qquad \text{Eq. (12)}$$

where E_m and E_f are the modulus of the matrix and the fiber, E_c is the storage modulus of the composite, Φ is an adjustable parameter. The parameter Φ could be related to the morphology of the composite. Comparison between the experimental results and the theoretical predictions gives a value of composite modulus of 16.4 GPa. The obtained value corroborates the experimental one. The parameter Φ determined from the data fit using the above equation, using the values of the neat matrix (2.2 GPa) and GF fiber modulus (70 GPa). The calculated parameter Φ was 0.986 indicating a higher efficiency of stress transfer between glass fibers and PPA matrix. Hence, the present manufacturing approach, which avoids some of the issues encountered with in-situ polymerization of reactive monomers [51], allow to preserving a relatively low viscosity compatible with liquid composite molding processes and to reach satisfactory mechanical properties.

Table 5: *Yield strength and flexural modulus of glass fiber-reinforced composites obtained at a reaction temperature of 280 °C. SD stands for standard deviation.*

	Yield strength (MPa)		Flexural modulus (GPa)	
Sample	σ (MPa)	SD (MPa)	E (GPa)	SD (GPa)
Neat PPA/CA	33.0	0.7	2.2	0.3
PPA/CA +60% GF	120.0	8.0	16.4	1.5

4. Conclusions

This article presents a new manufacturing method to prepare high Tg and melting temperature polyphtalamide thermoplastic polymer composites, using reactive extrusion of a low viscosity pre-polymer with a chain extender, injected into the mold containing the GF reinforcement, similar to RTM process. Firstly, the chain-extending reaction is demonstrated to be very rapid. Indeed, a series of adapted experimental studies have been performed to characterize the process and predict the processing window. Hereto, conventional ex-situ monitoring experiments (DSC, titration, rheometry and torque measurements) have shown that the reaction between PPA and CA agent occur at less than 2 min for which reason these techniques were unable to track the reaction at short times. Secondly, the reaction kinetics was therefore monitored using high temperature FTIR spectroscopy coupled to rheology. Subsequently, a rheo-kinetic model was established allowing to quantify the viscosity, especially at short times and therefore to predict the processing window for this kind of reactive PPA systems. Moreover, the modelled viscosity of this bi-component system was sufficient for filling and 30 seconds are a limit before rapidly rising. Interestingly, it was found that the evolution of the apparent conversion recorded by *in-situ* dielectric measurement during the process accurately matched the *ex-situ* counterpart obtained by FTIR coupled to rheology or by titration. Hence, it possible to achieve 85% of conversion at less than 2 minutes at the optimal reaction time of 280°C. The process could be under pressure (3-4 bar) and impregnation is helped with vacuum. Finally, high Tg PPA based composites were obtained with good impregnation properties. Overall, this study highlighted the potential of the High Temperature hybrid process (HT-ERTM) developed for this engineering polymer matrix. The obtained results demonstrated that the mechanical and thermomechanical properties of the resulting composites could be tuned through the control of processing parameters and especially time and reaction temperature. Hopefully, the present findings will provide a new guidelines for manufacturing PPA based composites for high service temperature applications in automotive and aerospace industries.

Acknowledgements

The authors acknowledge ARKEMA for providing the prepolymer and chain extender. The PhD thesis was performed in COMPOFAST project which was a framework of academic labs and many companies.

References

[1] F. Henning, L. Karger, D. Dorr, F.J. Schirmaier, J. Seuffert, A. Bernath, Fast processing and continuous simulation of automotive structural composite components, Composites Science and Technology 171 (2019) 261-279.
[2] P.E. Bourban, A. Bogli, F. Bonjour, J.A.E. Manson, Integrated processing of thermoplastic composites, Composites Science and Technology 58(5) (1998) 633-637.
[3] U.K. Vaidya, K.K. Chawla, Processing of fibre reinforced thermoplastic composites, International Materials Reviews 53(4) (2008) 185-218.
[4] J. Faraj, N. Boyard, B. Pignon, J.L. Bailleul, D. Delaunay, G. Orange, Crystallization kinetics of new low viscosity polyamides 66 for thermoplastic composites processing, Thermochimica Acta 624 (2016) 27-34.
[5] P. Cassagnau, V. Bounor-Legare, F. Fenouillot, Reactive processing of thermoplastic polymers: A review of the fundamental aspects, International Polymer Processing 22(3) (2007) 218-258.
[6] C.C. Hohne, R. Wendel, B. Kabisch, T. Anders, F. Henning, E. Kroke, Hexaphenoxycyclotriphosphazene as FR for CFR anionic PA6 via T-RTM: a study of mechanical and thermal properties, Fire and Materials 41(4) (2017) 291-306.
[7] N. Wiegand, E. Mader, Commingled Yarn Spinning for Thermoplastic/Glass Fiber Composites, Fibers 5(3) (2017).

[8] E. Archer, R. Mulligan, D. Dixon, S. Buchanan, G. Stewart, A.T. McIlhagger, An investigation into thermoplastic matrix 3D woven carbon fibre composites, Journal of Reinforced Plastics and Composites 31(13) (2012) 863-873.
[9] B.J. Kim, S.H. Cha, Y.B. Park, Ultra-high-speed processing of nanomaterial-reinforced woven carbon fiber/polyamide 6 composites using reactive thermoplastic resin transfer molding, Composites Part B-Engineering 143 (2018) 36-46.
[10] A. Luisier, P.E. Bourban, J.A.E. Manson, Initiation mechanisms of an anionic ring-opening polymerization of lactam-12, Journal of Polymer Science Part a-Polymer Chemistry 40(20) (2002) 3406-3415.
[11] P. Gerard, M. Glotin, G. Hochstetter, Composite material via in-situ polymerization of thermoplastic (meth)acrylic resins and its use, ARKEMA, Patent EP2985135, 2012.
[12] X. Ning, H. Ishida, RIM-pultrusion of nylon-6 and rubber-toughened nylon-6 composites, Polymer Engineering and Science 31(9) (1991) 632-637.
[13] S.K. Bhudolia, P. Perrotey, S.C. Joshi, Optimizing Polymer Infusion Process for Thin Ply Textile Composites with Novel Matrix System, Materials 10(3) (2017) 19.
[14] C. Williams, J. Summerscales, S. Grove, Resin infusion under flexible tooling (RIFT): A review, Composites Part a-Applied Science and Manufacturing 27(7) (1996) 517-524.
[15] S. Pillay, U.K. Vaidya, G.M. Janowski, Liquid molding of carbon fabric-reinforced nylon matrix composite laminates, Journal of Thermoplastic Composite Materials 18(6) (2005) 509-527.
[16] P.O. Mairtin, P. McDonnell, M.T. Connor, R. Eder, C.M. O Bradaigh, Process investigation of a liquid PA-12/carbon fibre moulding system, Composites Part a-Applied Science and Manufacturing 32(7) (2001) 915-923.
[17] A. Luisier, P.E. Bourban, J.A.E. Manson, Time-temperature-transformation diagram for reactive processing of polyamide 12, Journal of Applied Polymer Science 81(4) (2001) 963-972.
[18] L. Zingraff, V. Michaud, P.E. Bourban, J.A.E. Manson, Resin transfer moulding of anionically polymerised polyamide 12, Composites Part a-Applied Science and Manufacturing 36(12) (2005) 1675-1686.
[19] C. Hakme, I. Stevenson, A. Maazouz, P. Cassagnau, G. Boiteux, G. Seytre, In situ monitoring of cyclic butylene terephtalate polymerization by dielectric sensing, Journal of Non-Crystalline Solids 353(47-51) (2007) 4362-4365.
[20] A. Luisier, P.E. Bourban, J.A.E. Manson, Reaction injection pultrusion of PA12 composites: process and modelling, Composites Part a-Applied Science and Manufacturing 34(7) (2003) 583-595.
[21] P. Rosso, K. Friedrich, A. Wollny, R. Mulhaupt, A novel polyamide 12 polymerization system and its use for a LCM-process to produce CFRP, Journal of Thermoplastic Composite Materials 18(1) (2005) 77-90.
[22] T. Ageyeva, I. Sibikin, J. Karger-Kocsis, Polymers and Related Composites via Anionic Ring-Opening Polymerization of Lactams: Recent Developments and Future Trends, Polymers 10(4) (2018).
[23] A. Maazouz, K. Lamnawar, M. Dkier, Chemorheological study and in-situ monitoring of PA6 anionic-ring polymerization for RTM processing control, Composites Part a-Applied Science and Manufacturing 107 (2018) 235-247.
[24] T. Gratzl, Y. van Dijk, N. Schramm, L. Kroll, Influence of the automotive paint shop on mechanical properties of continuous fibre-reinforced thermoplastics, Composite Structures 208 (2019) 557-565.
[25] T.F. Novitsky, C.A. Lange, L.J. Mathias, S. Osborn, R. Ayotte, S. Manning, Eutectic melting behavior of polyamide 10,T-co-6,T and 12,T-co-6,T copolyterephthalamides, Polymer 51(11) (2010) 2417-2425.

[26] Capelot , M, G. Hochstetter, Reactive compositions made from thermoplastic amino prepolymer and unsaturated extender for thermoplastic composite materials**,** WO2017098181A1
[27] G. Hochstetter, J. Cauchois, H. Perrin, M. Glotin, Process for manufacturing a thermoplastic composite part in a closed mould, with injection into a cold mould, ARKEMA, Patent WO/2014/064377, 2014.
[28] S. Konstantopoulos, E. Fauster, R. Schledjewski, Monitoring the production of FRP composites: A review of in-line sensing methods, Express Polymer Letters 8(11) (2014) 823-840.
[29] E. Schmachtenberg, J.S. zur Heide, J. Topker, Application of ultrasonics for the process control of Resin Transfer Moulding (RTM), Polymer Testing 24(3) (2005) 330-338.
[30] M. Danisman, G. Tuncol, A. Kaynar, E.M. Sozer, Monitoring of resin flow in the resin transfer molding (RTM) process using point-voltage sensors, Composites Science and Technology 67(3-4) (2007) 367-379.
[31] Lin , D.J, Ottino , J. M, Thomas , E. L, A Kinetic study of the activated anionic polymerization of ε-caprolactam, Polymer Engineering and Science 25(18) (1985) 1155-1163.
[32] A. Maazouz, J. Dupuy, G. Seytre, Polyurethane and unsaturated polyester hybrid networks: Chemorheological and dielectric study for the resin transfer molding process (RTM), Polymer Engineering and Science 40(3) (2000) 690-701.
[33] A. Douhi, A. Fradet, Study of bulk chain coupling reactions. III. Reaction between bisoxazolines and carboxy-terminated oligomers, Journal of Polymer Science Part A: *Polymer Chemistry* 33(4) (1995) 691-699.
[34] Y. Sano, Polymerization of bis(2-oxazoline) compounds with dicarboxylic acids, Journal of Polymer Science Part A: Polymer Chemistry 27(8) (1989) 2749-2760.
[35] C. Vocke, U. Anttila, J. Seppala, Compatibilization of polyethylene polyamide 6 blends with oxazoline-functionalized polyethylene and styrene ethylene butylene styrene copolymer (SEBS), Journal of Applied Polymer Science 72(11) (1999) 1443-1450.
[36] M. Dkier, Etude rhéocinétique de polyamides HT: Application à la mise en forme de matériaux composites par des procédés réactifs, PhD Thesis, INSA Lyon, 2017.
[37] Y. Gabet, O. Gain, S. Al Akhrass, E. Espuche, G. Orange, Analysis and Optimization of fibre-matrix Interface in Glass-PA66 based Laminate Composites, Comptes rendus des vingtièmes Journées Nationales sur les Composites, JNC20, Paris (France), June 28-30, 2017.
[38] Pohl , H.A, Determination of Carboxyl End Groups in Polyester, Polyethylene Terephtalate, Analytical Chemistry 26(10) (1954) 1614-1616.
[39] Y. Tominaga, D. Shimamoto, Y. Hotta, Quantitative evaluation of interfacial adhesion between fiber and resin in carbon fiber/epoxy composite cured by semiconductor microwave device, Composite Interfaces 23(5) (2016) 395-404.
[40] C. Ramesh, A. Keller, S. Eltink, Studies on the crystallization and melting of nylon 66: 2. Crystallization behaviour and spherulitic morphology by optical microscopy, Polymer 35(24) (1994) 5293-5299.
[41] X.D. Fan, Y.L. Deng, J. Waterhouse, P. Pfromm, Synthesis and characterization of polyamide resins from soy-based dimer acids and different amides, Journal of Applied Polymer Science 68(2) (1998) 305-314.
[42] W. Meyer, F. Gentile, U. Suter, Rigid-rod fully aromatic polyamides with controlled constitution: synthesis and some properties, Macromolecules 24(3) (1991) 642-647.
[43] G. Rotter, H. Ishida, FTIR separation on nylon-6 chain conformations: Clarification of the mesomorphous and γ- crystalline phases, Journal of Polymer Science Part b-Polymer Physics 30(5) (1992) 489-495.
[44] S. Pichaud, X. Duteurtre, A. Fit, F. Stephan, A. Maazouz, J.P. Pascault, Chemorheological and dielectric study of epoxy-amine for processing control, Polymer International 48(12) (1999) 1205-1218.

[45] Kranbuehl , D, Delos , S, Yi , E, Mayer , J, Jarvie , T, Winfree , W, Hou , T, Dynamic dielectric analysis: Nondestructive material evaluation and cure cycle monitoring, Polymer Engineering and Science 26(5) (1986) 338-345.
[46] E. Szwajczakaf, A. Szymanski, On the relation Between Mobility of Ions and Viscosity. the Walden's Rule, Molecular Crystals and Liquid Crystals 139(3-4) (1986) 253-261.
[47] J.P. Southall, H. Hubbard, S.F. Johnston, V. Rogers, G.R. Davies, J.E. McIntyre, I.M. Ward, Ionic conductivity and viscosity correlations in liquid electrolytes for incorporation into PVDF gel electrolytes, Solid State Ionics 85(1-4) (1996) 51-60.
[48] G. Guerrero, M.B. Hagg, C. Simon, T. Peters, N. Rival, C. Denonville, CO2 Separation in Nanocomposite Membranes by the Addition of Amidine and Lactamide Functionalized POSS (R) Nanoparticles into a PVA Layer, Membranes 8(2) (2018).
[49] Z.A.M. Ishak, Y.W. Leong, M. Steeg, J. Karger-Kocsis, Mechanical properties of woven glass fabric reinforced in situ polymerized poly(butylene terephthalate) composites, Composites Science and Technology 67(3-4) (2007) 390-398.
[50] V.A. Alvarez, M.E. Valdez, A. Vazquez, Dynamic mechanical properties and interphase fiber/matrix evaluation of unidirectional glass fiber/epoxy composites, Polymer Testing 22(6) (2003) 611-615.

[51] K. van Rijswijk, H.E.N. Bersee, Reactive processing of textile fiber-reinforced thermoplastic composites - An overview, Composites Part a-Applied Science and Manufacturing 38(3) (2007) 666-681.

High Tg reactive PPA matrix

SAOS//FTIR

SAOS//DRS

Monitoring

Hybrid Processing

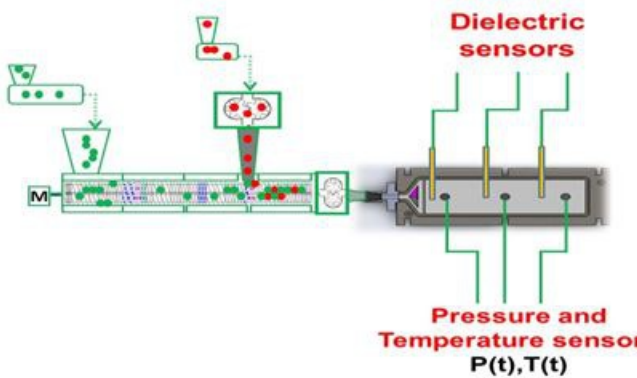

High-Performance PPA Composites

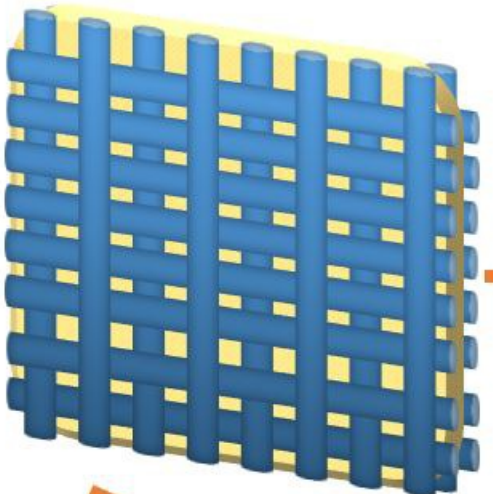

Thermomechanical performances